

# The potential of time-lapse GPR full-waveform inversion as high resolution imaging technique for salt, heat, and ethanol transport

P. Haruzi, IBG-3 FZ Jülich  
J. Schmäck, IBG-3 FZ Jülich  
L. Hain, IBG-3 FZ Jülich  
Z. Zhou, IBG-3 FZ Jülich  
R. Hoffmann, Liege University  
B. Pouladi, CNRS Rennes  
J. de La Bernardie, CNRS Rennes  
J. Vanderborcht, IBG-3 FZ Jülich  
H. Vereecken, IBG-3 FZ Jülich  
J. van der Kruk, IBG-3 FZ Jülich  
A. Klotzsche, IBG-3 FZ Jülich

**Keywords:** tracer test, GPR, full-waveform inversion, crosshole, hydrogeophysics.

## Introduction:

Time-lapse geophysical imaging of tracer tests is essential to infer preferential pathway characterization. Thereby, the mapping of small-scale heterogeneities within aquifers is crucial for characterizing flow and transport in the critical zone as realistic as possible. Compared to ray-based inversion methods for ground penetrating radar (GPR) data [1], the full-waveform inversion (FWI) of crosshole GPR data has shown a high potential to characterize soil properties of the near surface with a decimeter-scale resolution [2]. GPR FWI can provide high-resolution images of the geophysical properties relative dielectric permittivity  $\epsilon_r$  and electrical conductivity  $\sigma$ . The  $\epsilon_r$  can be linked to the aquifer porosity, and  $\sigma$  can be related to the pore fluid and clay content. Thus, tracers of different geophysical properties, which change (a) only electrical conductivity (e.g., salt [3]), and, (b) both electrical conductivity and permittivity (e.g., heat [4], ethanol [5]) are promising for GPR techniques.

In this regard, this abstract shows first a synthetic ethanol tracer test monitored by GPR FWI. As first step in the methodology, the synthetic tracer test is simulated and monitored by time-lapse crosshole GPR FWI, mimicking an experiment in typical aquifer conditions using a realistic aquifer model of the Krauthausen test site in Germany [6, 7]. Scenarios of different tracer types and magnitude of geophysical parameter changes are investigated. Thereby, different FWI starting models (SM) and two time-lapse FWI strategies are investigated to estimate the limitations of the techniques. The gained knowledge is used to perform real time-lapse GPR field measurements for several tracer tests. Field results, using for example heat as tracer (conducted at Krauthausen alluvial aquifer, site description in [6]), are preliminary interpreted in time-lapse by ray-based inversion and crosshole zero-offset (ZOP) attenuation analysis. In the next step, FWI will be applied on the GPR data with perspective whether it improves transport imaging resolution compared to other geophysical methods.

## Synthetic time-lapse GPR full-waveform inversion for monitoring ethanol tracer test:

Synthetic 3D flow and transport simulations (PARTRACE code, [8]) were used to generate a plume fate for synthetic GPR FWI modeling. Therefore, a lithological aquifer model with a cell size of 0.09 m was generated using sequential Gaussian simulation (SGEMS, [9]) software. Realistic widths of preferential paths (Figure 1f) were implemented by simulating log-conductivity, where the scale of heterogeneity is controlled by the vertical correlation length (CL) simulated with 0.18 m (derived from [6]). GPR property models ( $\epsilon_r$ ,  $\sigma$ ) were generated using a vertical CL of 0.12 m [7]. Such a CL can be challenging for the GPR resolvability, which is influenced by the wavelength physical limits [10] (dominant wavelength  $\lambda \sim 1.02$  m). As an example, we show the results for an ethanol tracer experiment. The geophysical properties of ethanol [5] were used ( $\epsilon_r$  and  $\sigma$  lower than of groundwater), to generate realistic GPR time-lapse changes. Synthetic 2D crosshole GPR data was simulated in background and time-lapse plume scenarios (Figure 1a,i;d,l) that will be used to perform the FWI. Thereby, different FWI starting model strategies for time-lapse data were tested to investigate which SM provides the most accurate plume reconstruction. As one result we observed that for a scenario with small  $\epsilon_r$  and  $\sigma$  changes caused by the tracer (here for ethanol max.  $\Delta\epsilon_r = -5$ ,  $\Delta\sigma = -8$ ), a SM that uses the background recovered  $\epsilon_r$  and the uniform average value of the  $\sigma$  (Figure 1c,j) provides the best reconstruction. Time-lapse independent FWI and double difference [11] FWI strategies show similar results (Figure 1g,h,o,p). For ethanol, the FWI is able to recover changes from both properties of about  $\Delta\epsilon_r = 1$  and  $\Delta\sigma = 1$  mS/m. Note that the  $\epsilon_r$  reconstruction tomograms are less smoothed than  $\sigma$  (Figure 1g,o), thus show a better potential to resolve preferential paths at  $\sim 0.1$  m scale.

## Field time-lapse GPR measurements for monitoring a heat tracer test, preliminary results:

Time-lapse crosshole GPR data was acquired during a natural gradient heat experiment at the Krauthausen test site using a multi-offset gather (MOG) setup with transmitter locations (Figure 2a, in circles) every 0.4 m, and receiver (crosses) every 0.1 m. For the heat tracer the time-lapse wave velocity (related to permittivity,  $v = c/\sqrt{\epsilon_r}$ ) of the ray-based inversion tomograms (Figure 2a) already indicate  $\epsilon_r$  temporal changes. As expected for an alluvial aquifer with low clay content, a positive feedback between wave velocity and temperature effect can be observed [4].

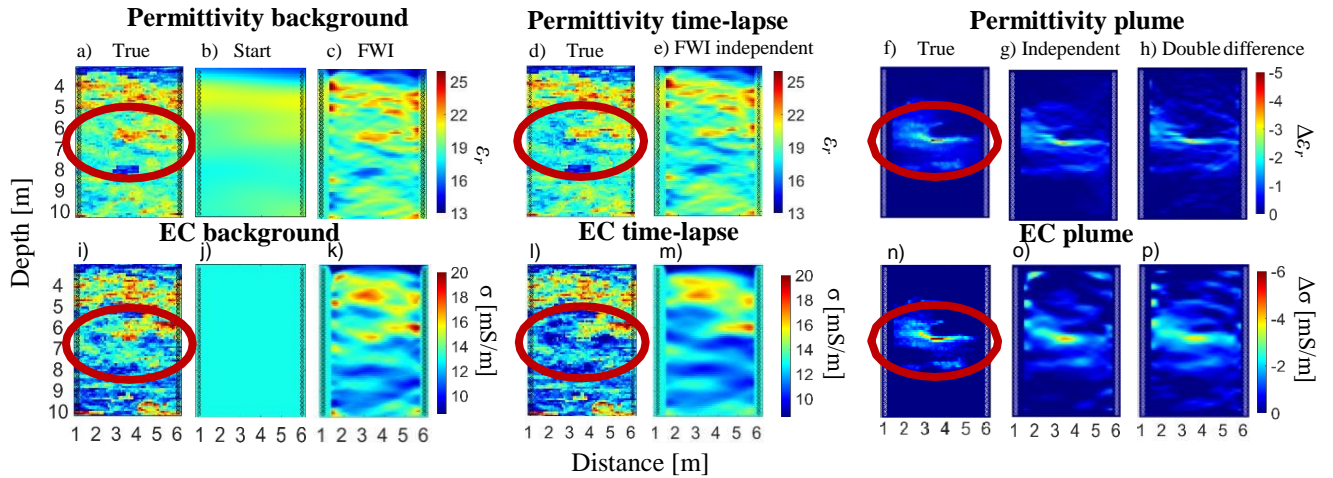


Figure 1: Ethanol plume reconstruction in a crosshole plane derived from synthetic GPR full-waveform inversion. True background (a,i) and time-lapse (d,l) permittivity and conductivity models are shown, while true permittivity and conductivity plume distribution is shown in (f) and (n). Red ellipses show the location of the plume. Starting models for background data inversion are smoothed background for permittivity (b) and uniform averaged conductivity (j). Starting models for time-lapse data inversion are the background recovered permittivity (c), and (j) for conductivity. Plume reconstructions from independent (g,o) time-lapse and background data inversions were performed by subtracting the FWI models (e,m) from the FWI background (c,k). Plume reconstruction using double-difference time-lapse strategy is shown in (h,p).

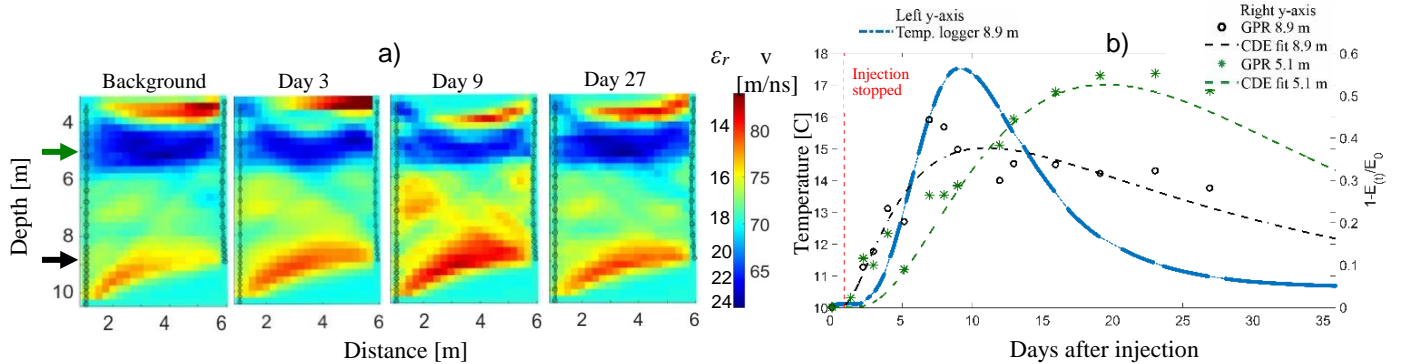


Figure 2: (a) Time-lapse crosshole GPR ray-based inversions of a field heat tracer at 5 m down-gradient for four different days. (b) Tracer breakthrough curves at 5 m down-gradient from a temperature logger at the left borehole in (a) at a depth of 8.9 (blue), and from a CDE fit (dashed curves) derived from GPR measurements (circles and asterisks), at 8.9 (black) and 5.1 m (green) depths (locations are shown with arrows in a). Temperatures of injected heat tracer and groundwater were 43.5 and 10.2 °C, respectively.

Below 4.5 m depth the electromagnetic wave velocity increases until day 9 by up to  $\Delta v \sim 5$  m/ns, and afterwards in day 27 decreases to nearly the recovered velocities (Figure 2a). Temperature logger data of a cased well located 5 m down-gradient from injection (Figure 2b, blue) shows a first temperature arrival after 2.58 days and the maximum temperature was measured 9.18 days after injection. This seems to agree with changes in the tomograms at depths below 4.5 m. Tracer breakthrough curves (BTC) were also derived from time-lapse GPR zero-offset trace attenuation ( $1 - \text{“GPR relative trace energy”}$ ) to provide 1D BTC depth profiles in 0.1 m intervals. They were fitted to the convection–dispersion equation (CDE) analytical solution [12] with  $R^2 = 0.88$  (Figure 2b), showing that this analysis is useful for monitoring the tracer in the plane. For a sand-gravelly layer at 8.9 m depth with a known [7] higher hydraulic conductivity, an earlier arrival of the heat tracer is observed than for a sandy layer at 5.1 m depth.

## Conclusions and outlook:

This study highlights the potential of time-lapse GPR full-waveform inversion as high resolution imaging technique for tracers of different geophysical properties. From first preliminary ray-based inversions using time-lapse field data, an approximation of permittivity changes can be derived. Also, simple attenuation analysis as depth profiles indicates major transport processes. But still ray-based or attenuation analysis are limited in expressing the tracer behavior, as fine heterogeneity is smoothed. As a realistic tracer quantification is required for robust transport, the study shows that enhanced geophysical methods like the time-lapse GPR FWI are promising to overcome these limitations and to come up with a high-resolution image of transport. FWI of acquired GPR field data consisting of two separate salt and heat tracer test will be used to apply FWI starting model strategies derived from the synthetics, and which will be tested for its resolution of transport imaging.

## References:

- [1] Holliger, K., Musil, M., & Maurer, H. R. (2001). *Ray-based amplitude tomography for crosshole georadar data: A numerical assessment*. Journal of Applied Geophysics, 47(3-4), 285-298.
- [2] Klotzsche, A., Vereecken, H., van der Kruk, J. (2019). *Review of crosshole ground-penetrating radar full-waveform inversion of experimental data: Recent developments, challenges, and pitfalls*. Geophysics, 84(6), H13-H28.
- [3] Giannakis, I. (2016). *Realistic numerical modelling of ground penetrating radar for landmine detection* (Doctoral dissertation, University of Edinburgh).
- [4] Seyfried, M. S., Grant, L. E. (2007). *Temperature Effects on Soil Dielectric Properties Measured at 50 MHz*. Vadose Zone Journal, 6(4), 759-765.
- [5] Glaser, D. R., Werkema, D. D., Versteeg, R. J., Henderson, R. D., Rucker, D. F. (2012). *Temporal GPR imaging of an ethanol release within a laboratory-scaled sand tank*. Journal of Applied Geophysics, 86, 133-145.
- [6] Englert, A. (2003). *Measurement, estimation and modelling of groundwater flow velocity at Krauthausen test site* (Doctoral dissertation, Bibliothek der RWTH Aachen).
- [7] Gueting, N., Vienken, T., Klotzsche, A., van der Kruk, J., Vanderborght, J., Caers, J., Vereecken, H., Englert, A. (2017), *High resolution aquifer characterization using crosshole GPR full-waveform tomography: Comparison with direct-push and tracer test data*. Water Resources Research, 53(1), 49-72.
- [8] Bechtold, M., Vanderborght, J., Weihermüller, L., Herbst, M., Günther, T., Ippisch, O., Kasteel, R., Vereecken, H. (2011). *Efficient random walk particle tracking algorithm for advective-dispersive transport in media with discontinuous dispersion coefficients and water contents*. Water Resources Research, 47(10).
- [9] Remy, N., Boucher, A., & Wu, J. (2009). *Applied geostatistics with SGeMS: a user's guide*. Cambridge University Press.
- [10] Oberröhrmann, M., Klotzsche, A., Vereecken, H., van der Kruk, J. (2013). *Optimization of acquisition setup for cross-hole GPR full-waveform inversion using checkerboard analysis*. Near Surface Geophysics, 11(2), 197-209.
- [11] Asnaashari, A., Brossier, R., Garambois, S., Audebert, F., Thore, P., Virieux, J. (2015). *Time-lapse seismic imaging using regularized full-waveform inversion with a prior model: which strategy?*. Geophysical prospecting, 63(1), 78-98.
- [12] Kemna, A., Vanderborght, J., Kulesa, B., & Vereecken, H. (2002). *Imaging and characterisation of subsurface solute transport using electrical resistivity tomography (ERT) and equivalent transport models*. Journal of Hydrology, 267(3-4), 125-146.

## Acknowledgements:

This study is part of the Enigma ITN program (European training Network for in situ imaging of dynamic processes in heterogeneous subsurface environments). This project has received funding from the European Union's Horizon 2020 research and innovation programme under the Marie Skłodowska-Curie Grant Agreement No. 722028.